Electrocatalytic Oxidation of L-cysteine by Adamantane Ester Schiff Base Nickel Complexes

Hao Wang[1], Zheng Liu[1,], Qiuqun Liang[1], Guo-Cheng Han[2,*], Peng Guo[1], Xinqiao Lao[1], Shufen Zhang[1,3], Zhencheng Chen[2], Ruosheng Zeng[2]*

[1] College of Chemical and Biological Engineering, Guilin University of Technology, Guilin 541004, P.R. China
[2] School of Life and Environmental Sciences, Guilin University of Electronic Technology, Guilin, 541004, P.R. China
[3] State Key Laboratory of Fine Chemicals, Dalian University of Technology, Dalian 116024, P. R. China
[*] E-mail: lisa4.6@163.com, hangc1981@163.com

A p-aldehyde benzoic acid adamantine ester (D1), 4-formyl benzoic acid adamantane ester shrinking o-aminophenol Schiff base (D2) and its nickel complexes (D3) were synthesized and characterized by thermogravimetric analysis, H^1-NMR and UV-Vis spectrum. A glassy carbon electrode was chemically modified by adamantine esters Schiff base nickel complexes which was employed for determination of L-cysteine. The influences of the effective parameters such as the pH of supporting electrolyte, scanning rate and the time of maceration adsorption were investigated. The electrochemical responses to L-cysteine have a good linearity in the range of 0.01 and 0.08 mmol/L with the detection limit of 5.0 μmol/L. The recovery rate was between 97.88% and 101.96% with the relative standard deviation of 3.9%. Therefore, a new detection method for the L-cysteine content had been established in food based on Schiff base nickel complexes.

1. INTRODUCTION

L-cysteine is an important sulfur-containing amino acid with bioactivity [1-3]. L-cysteine has a significant physiological function on animals' nutrition and immunity for its unique structure [4,5]. Many functional enzymes have some relevance to its -SH within cysteine. What's more, cysteine has been widely used in food industry, pharmaceutical factory, beauty industry and feed production. Thus, a novel and simple detection method for L-crysteine is eager to be established [6-9].

Up to now, the detection methods quantitatively for L-cysteine include spectrophotometry [10,11], HPLC [12-14], chemiluminescence [15,16], voltammetry [17], liquid chromatography-mass spectrometry (LC-MC) [18] and enzyme-linked immunosorbent assay (ELISA) [19]. However, the voltammetry method is passionately pursed because of its easy production, easy operation, safe and green environmental protection. It has been reported that the way of electrode modification could endow plenty of new functions by self-assembly, drop-coating, covalent bonding, electrodeposition or activated absorption [20-25]. Wang and coworkers [26] used modified glassy carbon electrodes, which mesoporous molecular sieves filled with nickel and cobalt complexes, to test its electrochemical performance by cyclic voltammetry, chronoamperometry and chronocoulometry. The results showed that the modified electrodes had a good effect on the electrocatalysis of alcohol. And Mirha Pazalja and coworkers [27] put forward a new low potential electrochemical sensor for determination of L-cysteine based on carbon electrodes modified with Ru(III) Schiff base complex, multi-walled carbon nanotubes and nafion. Therefore, the modified electrodes can be used to analyze the contents and properties of the pharmaceutical products by electrochemical methods[28].

Schiff base can be generated from the condensation reaction between substances containing –C=O and -NH$_2$. The C=N double bonds in the molecules of the Schiff base can coordinate with metal ions and form conjugated structure with other unsaturated groups. Different steric hindrances and various functional groups can be introduced on its side in order to change the property of the Schiff base compounds [29-32]. Due to the characteristic of the coordination, Schiff base compounds are widely applied to catalysis [33], medication [34] and photoelectric materials [35] and other fields nowadays. Furthermore, the electric analysis of Schiff base derivatives is very popular [36-38].

Mashkoor [39] provided a new method about electrochemical determination of L-cysteine by an elbow shaped, Sb-doped ZnO nanowire-modified electrode. It shows excellent electrochemical properties such as low detection limit and favorable stability. Palanisamy [40] used gold-5-amino-2-mercapto-1,3,4-thoadiazole core-shell nanoparticles film modified electrode to test the detection of L-cysteine. It showed better recoveries for spiked L-cysteine into blood serum and urine and had a detection limit of 3 pM. Chunyan Deng [41] constructed a boron-doped carbon nanotube-modified glassy carbon electrode to measure the content of L-cysteine. It exhibited a good resistance against interference by other oxidizable amino acids.

In this article, a simple and efficient route is to prepare the Schiff base complexes in combination with nickel. The electrodes will be modified by the prepared Schiff base complexes which have electrochemical behavior towards detecting the content of L-cysteine.

2. EXPERIMENTAL

2.1 Reagents and Apparatus

L-cysteine was purchased from Guangfu Fine Chemical Research Institute (Shanghai, China). N, N-dimethyl formamide was purchased from Xilong Chemical Research Co. (Shantou, China) and graphite oxide graphene from Lelo Biological Technology Co., China. All the chemical reagents were

of analytical grade and used as received. 4-formyl benzoic acid adamantane ester shrinking o-aminophenol Schiff base nickel complexes was self-synthesized. Distilled water was used as solvent to prepare all solutions.

The UV-Vis spectra were recorded on a UV-2450 spectrophotometer (Shimadzu, Japan). The H[1]-NMR test was performed on AUANCE Av500Hz nuclear magnetic resonance spectrum instrument (Bruker, Switzerland). The thermogravimetric tests were carried out on STA-99 thermal gravimetric analyzer (NETZSCH Co., German). The IR spectra were studied on FTIR-8400 spectrometer (Shimadzu Co., Japan). The electrochemical tests were taken on CHI660D electrochemical workstation (Beijing Branch Putian Technology Co., China).

2.2 Synthesis of the Adamantane esters Schiff base nickel complexes

2.2.1 Preparation of adamantane ester

A powder of 0.5 g (0.0033 mol) 4-formylbenzoic acid was dissolved in 0.608 g (0.004 mol) adamantane alcohol in a 100 mL single port flask, a powder of 0.858 g dicyclohexyl carbodiimide(DCC) and 0.067 g 4-dimethyl amino pyridine(DMA) were added. After vacuuming 30 min by oil pump, 30 mL anhydrous dichloromethane was added to the flask with stirring 8 h under the nitrogen atmosphere, white precipitate of dicyclohexyl urea (DCU) was prepared. After purification, white powder denoted as D1 was obtained for use. IR ν_{max} (KBr), 1701 cm^{-1} (C=O, ester group), 3022 cm^{-1} (C–H, benzene ring), 3447 cm^{-1} (O–H, benzene ring), 1263 cm^{-1} (C–N, benzene ring). H[1]-NMR (500 MHz, CDCl$_3$, ppm) δ: 10.10 (s, 1H, multiplet), 8.19-8.10 (m, 2H, multiplet), 7.93 (dd, J = 7.4, 1.2 Hz, 2H, multiplet), 2.27 (d, J = 13.8 Hz, 9H, multiplet), 1.79-1.68 (m, 6H, multiplet).

2.2.2 Synthesis of ligands

A powder of 0.5 g 4-formylbenzoic acid adamantane ester was dissolved in 20 mL anhydrous ethanol in a single port flask, a solution of 0.19 g ortho-aminophenol in 10 mL anhydrous ethanol and 6 to 8 drops glacial acetic acid were added dropwise. After stirring 5 h under the nitrogen atmosphere, a great many yellow precipitate was prepared. The yellow production prepared above was cooled and filtered after stewing. And then the colored product recrystallized from absolute ethanol and dried until pure yellow powder of 4-formyl benzoic acid adamantane ester shrinking o-aminophenol Schiff base denoted as D2 was obtained for use. IR ν_{max} (KBr), 3083 cm^{-1} (C–H, benzene ring), 1630 cm^{-1} (C=N, benzene ring). H[1]-NMR (500 MHz, CDCl$_3$, ppm) δ: 8.77 (s, 1H, multiplet), 8.11 (d, J= 8.3 Hz, 2H, multiplet), 7.97 (d, J = 8.3 Hz, 2H, multiplet), 7.35 (dd, J = 8.1, 1.3 Hz, 1H, multiplet), 7.24 (dd, J = 10.1, 2.8 Hz, 1H, multiplet), 7.05 (dd, J = 8.1, 1.2 Hz, 1H, multiplet), 1.75 (q, J = 12.6 Hz, 9H, multiplet), 1.59 (s, 6H, multiplet).

2.2.3 Synthesis of nickel complexes

The 0.5 g of 4-formyl benzoic acid adamantine ester shrinking o-aminophenol Schiff base was added to the mixture consisting of absolute ethanol and N, N-dimethyl formamide(DMF) with the volume ratio of 6:1 and the total amount of 35 mL. The 10 mL of absolute ethanol solution contained 0.117 g nickel acetate was dribbled into the reaction mixture stirring at the temperature of 65°C laxly. After refluxing for 3 h, the dark yellow precipitate production was generated. The dark yellow production was filtered after stewing. The product was recrystallized by absolute ethanol and dried for the purpose of obtaining the dark yellow powder nominated 4-formyl benzoic acid adamantane ester shrinking o-aminophenol Schiff base nickel complexes denoted as D3. IR v_{max} (KBr), 3083 cm^{-1} (C–H, benzene ring), 1621 cm^{-1} (C=N, benzene ring), 400 cm^{-1} (Ni–O), 700 cm^{-1} (Ni–N).
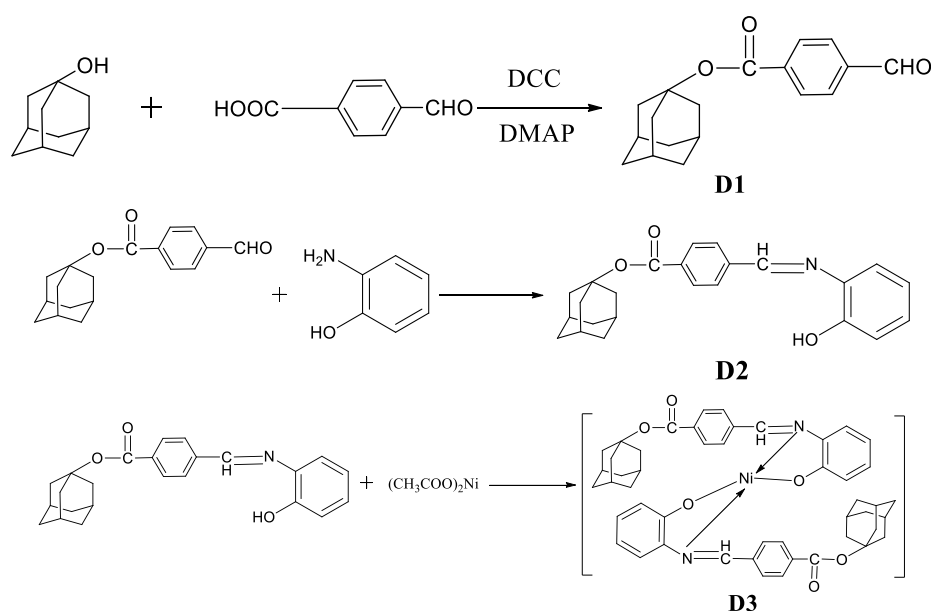
Scheme 1. Synthesis route of D1, D2 and D3

2.3 Preparation of Ni (II)/graphene oxide/glassy carbon modified electrodes and electrochemical measurement.

Modified electrodes were prepared by the process that polished, ultrasonic treatment, coated and settled. Prior to the electrode modification, the bare glassy carbon electrode surface was polished with aluminum powder and then sonicated in deionized water, ethanol and redistilled water. Right after, 1 mL DMF solvent was added to 1mg graphene oxide ultrasonically vibrating till the mixture became the black suspension. And 5 μL graphene oxide suspension was coated on the surface of a glassy carbon electrode, which was naturally volatile at the room temperature. In addition, the surface of graphene/glassy carbon electrode was coated by 5 μL (2.0 mmol/L) DMF solution consisting of D3 in multiple times up to 6 times in order that the solution on the electrode surface was considered as a nature adsorption. And then the electrode was aired at the room temperature about 1 h before rinsing

with distilled water to remove the substances which were not adsorbed on the surface. According to the steps mentioned above, a glassy carbon electrode modified by D3 and graphene oxide was obtained.

The electrochemical tests of nickel complexes were carried out with 0.2 mol/L PBS buffer solution (pH=7.0) as solvent in a common three-electrode system using modified electrode as working electrode, platinum wire as auxiliary electrode and Ag/AgCl as reference electrode at a scanning speed of 50 mV s^{-1} with the potential window ranging from -1.00 to 0.60 V at room temperature. Besides, the modified electrode was soaked in different concentration L-cysteine solution for 30 min before electrochemical measurement.

3. RESULTS AND DISCUSSION
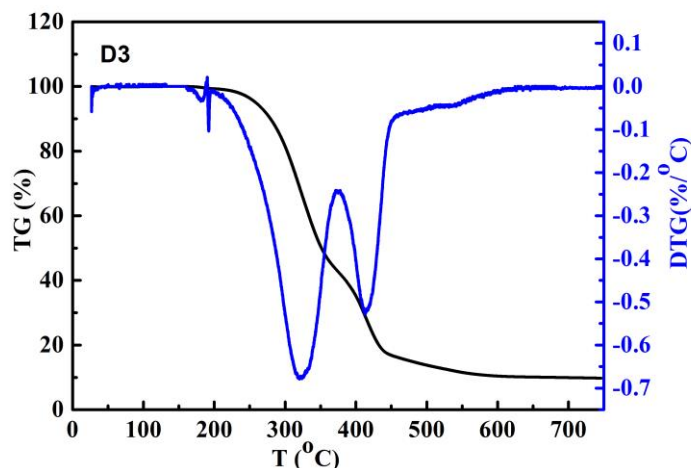
3.1 Thermogravimetric analysis.
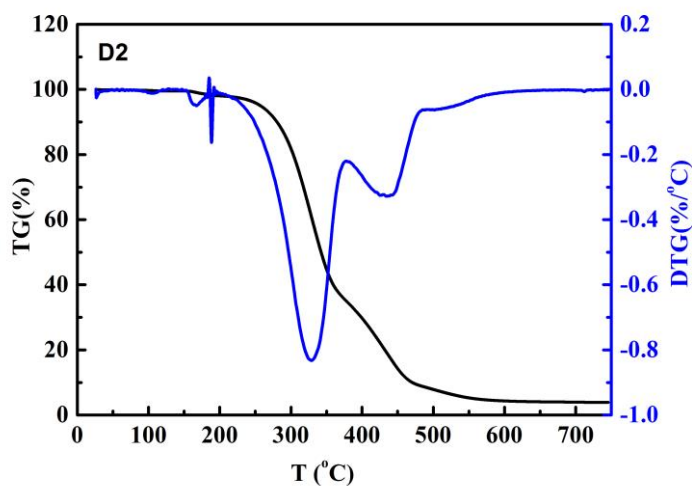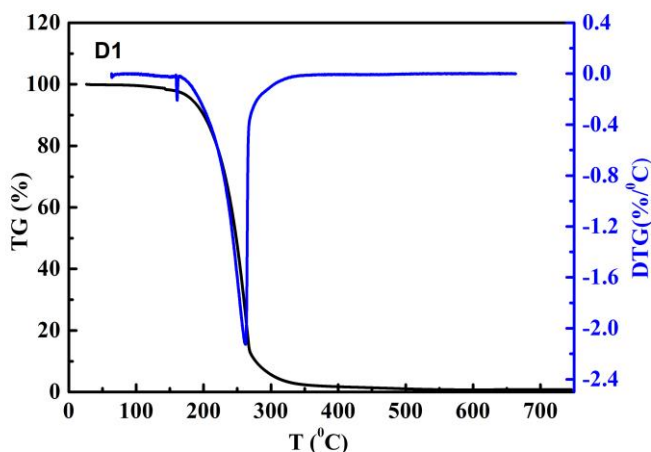
Figure 1. TG curves of (D1) p-aldehyde benzoic acid adamantine ester, (D2) 4-formyl benzoic acid adamantane ester shrinking o-aminophenol Schiff base and (D3) nickel complexes of D2

The thermal decomposition process of the products can be comprehended by the thermal analysis of the products, substance structure and heat stability at the applicable temperature range. The results are shown in Figure 1.

The thermal analysis of D1 shows initially a platform before 165°C which confirms 4-formyl benzoic acid adamantine ester don't decomposed. When the temperature exceeds 165°C, the curve has a significant decline due to the decompositions [42]. In addition, the residual rate has been close to 0 till the temperature of 350°C indicates that D1 has been decomposed completely. Curves D2 and D3 are similar to curve D1 shows that a platform before 200°C. When the temperature exceeds 200°C, the curve has a significant decline due to the decompositions of D2 or D3. The difference between Curve D1 and D2 is that the temperature of D2's complete decomposition is 550°C. Besides, when the temperature has reached to 560°C, the TG curve of D3 appears a platform again and the residual rate of D3 is 10% [43]. According to the common knowledge of nickel complexes, this residual material should be nickel oxide [44]. The theoretical calculation value is calculated by 9.30% which is close to the actual residue. Comparing the three substances, the order of the thermal stability is D3 >D2> D1.

3.2 UV-vis Spectrum Analysis.

The UV-vis results show that 4-formyl acid adamantane ester, its Schiff base and nickel complexes (D1, D2 and D3) have their unique absorption peaks. As shown in Fig.2, the absorption peak is located at about 275 nm of the three substances for the reason of the benzene ring with B(π~π*electron transition) [45]. The absorption peaks of D2 and D3 are situated at 376 nm and 374 nm because of the n~π* electron transition of C = N conjugated to benzene ring [46].
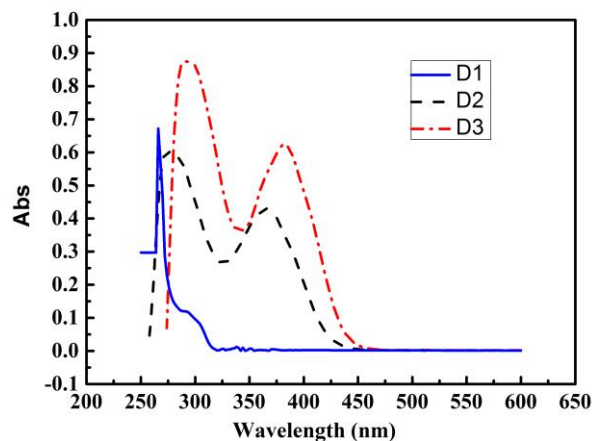
Figure 2. UV-vis Spectrum of (D1) p-aldehyde benzoic acid adamantine ester (D2) 4-formyl benzoic acid adamantane ester shrinking o-aminophenol Schiff base (D3) nickel complexes of D2 in DMF solution with the concentration of 10.0 μmol/L

3.3 Electrochemical properties of complexes.

It can be obvious seen in Fig.3 that the curve demonstrated a couple of reversible redox peaks within the potential window of -0.8 to 0.4 V, which belongs to the electrode reaction of Ni(III)/Ni(II) at a scanning speed of 50 mV s^{-1}.The potential of oxidation and reduction peak is -0.266 V and -0.396 V respectively, so the potential difference can be calculated with a value of 0.13 V. It can be indicted that D3 has a good electrochemical property due to the good cyclic reversibility of the electrode reaction.
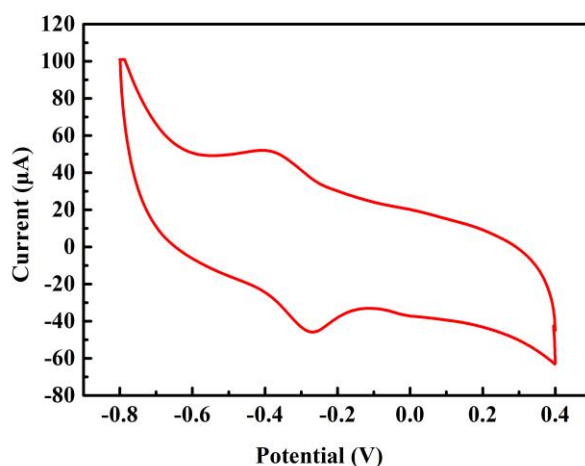

Figure 3. The cyclic voltammetry graph of p-formyl benzoic acid adamantane ester shrinking o-aminophenyl nickel complexes solution (0.02 mmol/L D3) with Ni complexes/graphene oxide/glassy carbon modified electrode at the scanning rate of 50 mV/s in 0.2 mol/L PBS solution

3.4 Electrochemical performance study of the Ni complexes/graphene oxide/glassy carbon modified electrode

3.4.1 The cyclic voltammetry performance of L-cysteine by using glassy carbon electrodes modified by Ni complexes/graphene oxide.
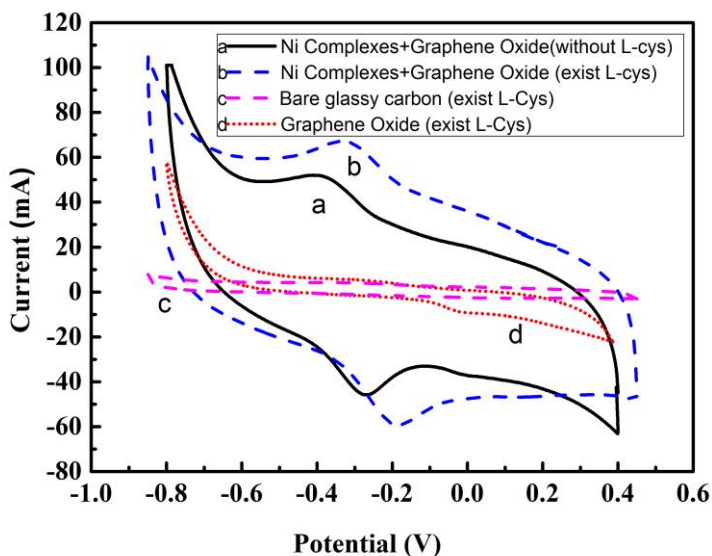

Figure 4. The cyclic voltammetry graph of 0.02 mol/L L-cysteine in 0.2 mol/L PBS solution with different electrodes

According to the preparation method of modified electrodes mentioned above, the glassy carbon electrodes modified by graphene oxide or Ni complexes/graphene oxide were produced respectively. And the results of different electrodes modified by Ni complexes and graphene oxide without L-cysteine (Curve b), Ni complexes and graphene oxide existing L-cysteine (Curve a), bare glassy carbon with L-cysteine (Curve c) and graphene oxide existing L-cysteine (Curve d) respectively were shown in Fig.4.

It can be obvious seen in Fig.4 that the Curve c and d show no oxidation peaks and reduction peaks, which indicates that L-cysteine is difficult to be oxidized and reduced in nature. And the Curve a and b show a pair of Faradic peaks belonged to the electrode reaction of Ni(III)/Ni(II). In comparison, the peak intensity of b is stronger than a. The reason is due to the addition of L-cysteine. It is indicated that L-cysteine on glassy carbon electrodes modified by Ni complexes/graphene oxide are easily oxidized due to the electronic media role of nickel complexes and large specific surface area of the oxide graphene [47].

3.4.2 The choice of the supporting electrolyte PBS buffer's pH.

The cyclic voltammetric response effect for L-cysteine in different pH of PBS buffer solutions with the value of pH was 6 to 8 respectively was tested. The result of the test was shown in Fig.5. It is

indicated that the intensity and the area of the oxidation peak tested in PBS buffer solution which pH= 7 is the largest among the three samples. The conclusion that the PBS buffer solution of pH=7 is more suitable to be the supporting electrolyte.
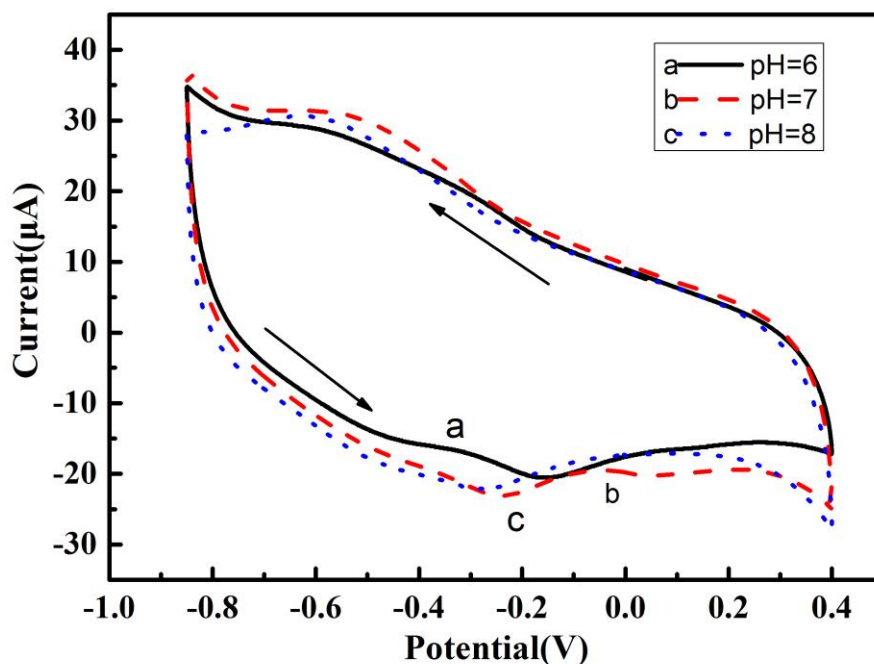

Figure 5. The cyclic voltammetry curves of 0.02 mmol/L L-cysteine solution in different pH of 0.2 mol/L PBS solution with Ni complexes/graphene oxide/glassy carbon modified electrode (The arrow shows the direction of scan)

3.4.3 Effect of scanning rate on oxidation peak current.

It was investigated that the effect of scanning speed on the oxidation peak current shown in Fig.6 [48]. It is clearly seen that the current of the oxidation peak increased with the crescent scanning rate in proportion basically which linear equation is $y=-5.10408e^{-6}-5.3135e^{-7}*x$ with the linear correlation coefficient of 0.9960, which is indicated that the oxidation process of L-cysteine in the modified electrode is controlled by adsorption. It can be further explained that the adsorption process that L-cysteine in the surface of the glassy carbon electrode modified by nickel complexes/oxide graphene is the controlling step of the whole electrode reaction [49]. Therefore it is significant to measure the accurate result that the accumulation time of impregnating the modified electrode into the L-cysteine.
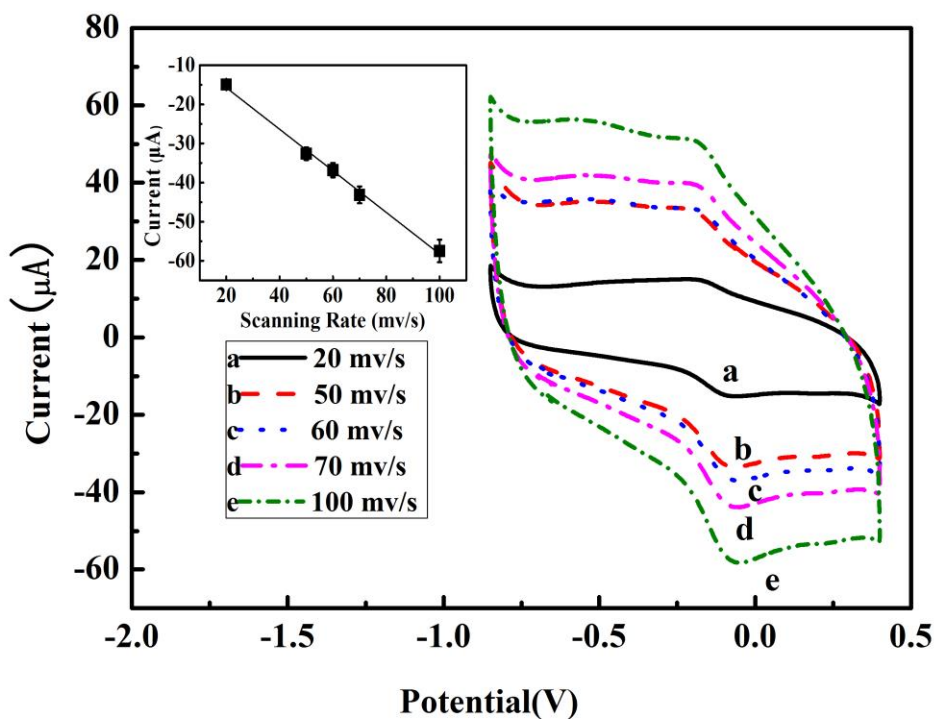
Figure 6. The cyclic voltammetry curves of 0.02 mmol/L L-cysteine solution at different scan rates of 0.2 mol/L PBS solution with Ni complexes/graphene oxide/glassy carbon modified electrode

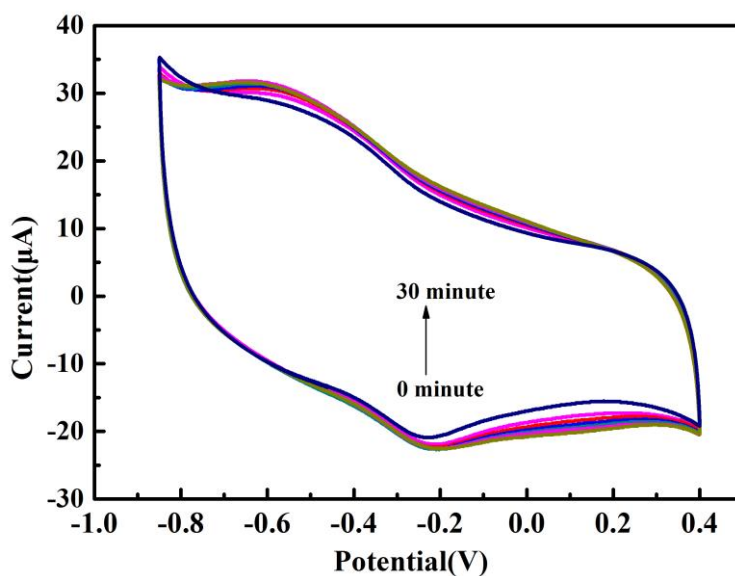*3.4.4 Effect of impregnation time.*

Figure 7. The cyclic voltammetry curves of Ni complexes/graphene oxide/glassy carbon modified electrodes immersed in different time of L-cysteine

The cyclic voltammetry curves were measured in 0.06 mmol/L PBS buffer solution (pH=7) after dipping the modified electrodes into L-cysteine for different time, which the dipping time was gradient for 5 minutes from 0 to 30 minutes, shown in Fig.7. It is indicated that the current of the modified electrodes in PBS buffer solution has been increased with the extension of dipping time. Moreover, it is further suggested that the modified electrodes have adsorption on L-cysteine [50]. Over time, the concentration of L-cysteine adsorbed on the electrode surface is rising that leads to the peak current increasing gradually. It can be seen clearly that as the time of adsorption extended further, the variation of the current has a tendency to reduce, such as 30 min. We can infer that the cause of the above phenomenon is adsorption saturation of the electrodes.
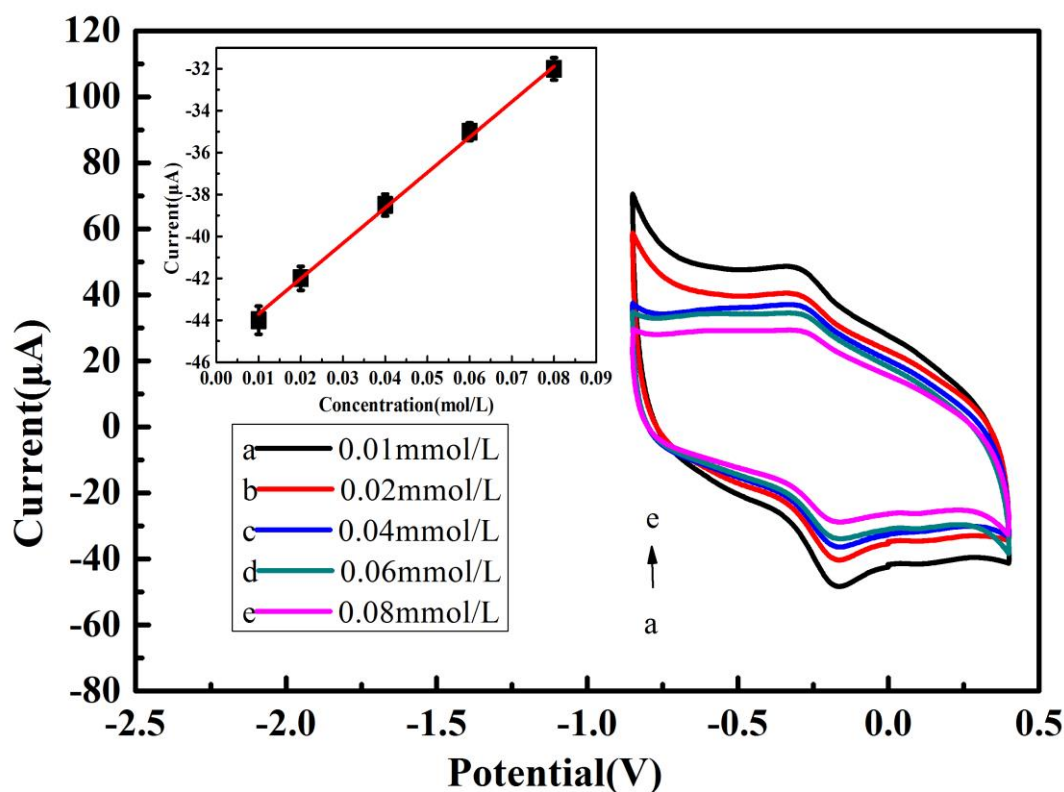
3.4.5 Working curve

Figure 8. The cyclic voltammetry in different concentrations of L-cysteine on the Ni complexes/graphene oxide/glassy carbon modified electrode and its working curve

Cyclic voltammetry was performed by using the modified glassy carbon electrode in the different concentration of L-cysteine shown in Fig.8. It is observed clearly that as the increasing concentration of L-cysteine, the current of redox peak had been decreased. The occurrence of this phenomenon is probably due to the coordination between nickel ions and the L-cysteine that has an effect on electrochemical activity of nickel complexes to a certain degree [51,52]. L-cysteine has

strong coordination ability, which can coordinate with nickel ions in the electron media of adamantane schiff-base nickel complexes which are modified on the electrode, so that the electron transfer ability of the modified electrode is decreased and lead to the decreased current signal. In addition, the concentration of L-cysteine ranging from 0.01 to 0.08 mmol/L has a good linear relation with the current value of oxidation peak which linear equation is y=-4.53963e^{-5}+1.71341e^{-4}*x with a linear correlation coefficient of 0.99303 [53]. Besides, the detection limit calculated by the equation $LOD = \dfrac{3\alpha}{S}$ was 5.0 μmol/L.

Table.1 shows the electrochemical determination methods of L-cysteine with different chemical modified electrodes. It can be seen that although the sensitivity (0.0294 μA/μM) of this experiment is lower, the use of adamantane schiff base nickel complexes as electron media in chemical modified electrodes expands the application of schiff bases.

Table 1. Comparision of chemical modified electrodes for L-cysteine determination

Electrode material	Analyte	Detection limit	Linear range	Correlation	Sensitivity	References
Sb-doped ZnO nanowire	L-Cysteine	0.025 μM	0.075-100 μM	——	400 nA/μM	[39]
GNF	L-Cysteine	3 pM	10-140 nM	——	——	[40]
Boron-doped carbon nanotube	L-Cysteine	0.26 μM	0.78-200 μM	0.998	25.3 nA/mM	[41]
DNO	L-Cysteine	0.07 μM	——	0.9988	44 μM/mM	[53]
Electrospun carbon nanofibers	L-Cysteine	0.1 μM	0.15-64 μM	0.9996	——	[54]
Hollow cubic cuprous oxide	L-Cysteine	2.3 μM	6.0-100 μM	0.9933	——	[55]
MCB	L-Cysteine	45.87 nM	50-700μM	——	0.0097 μA/μM	[56]
Adamantane Ester Schiff Base Nickel Complexes	L-Cysteine	5.0 μm	0.01-0.08mM	0.99303	0.0294 μA/μM	this work

GNF:Gold-5-amino-2-mercapto-1,3,4-thiadiazole core-shell nanoparticle film; DNO:DNA/nickel oxide nanoparticles/osmium (III); MCB:Metal impurity containing carbon black

3.4.6 Interference experiment.

The interference experiment was tested by controlling the relative error in the plus or minus 5%. It is a small volume of high concentration of interference ions that was added to 5 mL of 0.001 mmol/L PBS buffer solution consisting of L-cysteine. The results show that when the determination of the relative error less than 5%, 10 times the concentration of threonine, serine, glycine, valine, L-tyrosine and citric acid or 100 times of sodium ions, chloride ions, sulfate ions and phosphate didn't interfere with the determination of L-cysteine with the proposed method as shown in Table 2.

Table 2. The interference experiment with determination of L-cysteine

Materials	Times	Relative error
Threonine	10	4.2%
Serine	10	3.5%
Glycine	10	3.7%
Valine	10	2.9%
L-tyrosine	10	3.5%
Citric acid	10	2.7%
NaCl	100	4.6%
Na_2SO_4	100	4.8%
Na_3PO_4	100	4.6%

3.4.7 Reproducibility and stability of the modified electrodes.

The stability of the modified electrode was determined with the method of the cyclic voltammetry with the potential window ranging from -0.85 to 0.40 V in 0.02 mol/L L-cysteine solution. The results show that the peak height of the cyclic voltammetry curve is not significantly changed after 100 cycles at the scanning rate of 50 mV/s. The standard relative error was 2.87% measuring continuously in the solution of L-cysteine mentioned above indicating that the modified electrode has a good repeatability and stability.

3.4.8 Analytical application.

Table 3. Determination of L-cysteine content in milk samples

Samples	Measured value mmol/L (n=5)	RSD	Adding standard recovery experiment			
			Background value g/L	Additive scalar g/L	Total g/L	Recovery rate %
Milk	0.01429	3.9%	0.00173	0.0002	0.00192	99.70
			0.00173	0.0002	0.00189	97.88
			0.00173	0.0002	0.01709	98.83
			0.00173	0.0002	0.00196	101.96
			0.00173	0.0002	0.00190	98.56

For the application of the modified electrode, the method of spiking recovery were used to detect the content of L-cysteine in milk. A solution of 5 mL commercially available milk samples which was boiled until anaerobic was added to PBS buffer solution which pH=7 diluting it to 25 mL

after cooling. Then the determination of L-cysteine was tested. To a solution of 5 mL processed milk in 20 mL PBS buffer solution was added a certain amount of L-cysteine standard solution tested by recovery experiments shown in Table.3. It is clearly seen that the relative standard deviation (RSD) is 3.9% and the standard recovery rate is between 97.88% and 101.96% indicated the good precision and the accuracy of the method.

4. CONCLUSION

This work described that a glassy carbon electrode was modified by Schiff base nickel complexes-graphene oxide (Ni-GO) and used for determination of L-cysteine. It concluded that electronic media effect of the nickel complexes and larger specific surface area of the graphene oxide result from L-cysteine had a good cyclic voltammetry behavior on the modified electrodes. The modified electrode was suitable to assay the content of L-cysteine, a new method for measuring the content of L-cysteine was established, which was simple manufacture, convenient operation, safety and environmental protection.

References

1. T.W. Hart, *Tetrahedron Lett.,* 26 (1985) 2013.
2. L. Zheng, R.H. White, V.L. Cash, and D.R. Dean, *Biochemistry-US,* 33 (1994) 4714.
3. P. Olhoft, and D. Somers, *Plant Cell Rep.,* 20 (2001) 706.
4. N.K. Özer, S. Taha, and A. Azzi, *Biofactors*, 24 (2005) 193.
5. S.G. Ge, M. Yan, J.J. Lu, M. Zhang, F. Yu, J.H. Yu, X.R. Song, and S.L. Yu, *Biosens. Bioelectron.*, 31 (2012) 49.
6. W.S. Zhou, C.H. Li, and C. Sun, *Food Chem.*, 192 (2016) 351.
7. S. Shankar, and S.A John, *Sensor. Actuat. B-Chem.*, 221 (2015) 1202.
8. L. Zhang, L. Ning, Z.F. Zhang, S.B. Li, H. Yan, H.J. Pang, and H.Y. Ma, *Sensor. Actuat. B-Chem.*, 221 (2015) 28.
9. M. Amjadi, Z. Abolghasemi-Fakhri, and T. Hallaj, *J. Photoch. Photobio. A-Chem.,* 309 (2015) 8.
10. A. Besada, N.B. Todros, and Y.A. Gawargious, *Microchimi. Acta*, 99 (1989) 143.
11. A.S. Dimas, C.L. Kelly, T.B. Gassia, *Talanta*, 50 (1999) 1003.
12. H. Birwé, and A. Hesse, *Clin. Chim. Acta*, 199 (1991) 33.
13. K.S. Yoo, and L.M. Pike, *Sci. Hortic-Amsterdam*, 75 (1998) 1.
14. Y.W. Wang, S. Tang, H.H. Yang, and H. Song, *Talanta*, 146 (2016) 71.

15. P. Yang, Y.H. Chen, Q.Y. Zhu, F.W. Wang, L. Wang, and Y.X. Li, *Microchim. Acta*, 163 (2008) 263.
16. X. Xu, J. Qiao, N. Li, and S. Zhang, *Anal. Chim. Acta,* 879 (2015) 97.
17. B. Yosypchuk, and L. Novotný, *Talanta,* 56 (2002) 971.
18. X. Guan, B. Hoffman, C. Dwivedi, and D.P. Matthees, *J. Pharmaceut. Biomed.*, 21 (2003) 251.
19. L. Udby, J.B. Cowland, A.H. Johnsen, O.E. Sorensen, N. Borregaard, and L. Kjeldsen, *J. Immunol. Methods*, 263 (2002) 43.
20. D. Merli, F. Ravasio, S. Protti, M. Pesavento, and A. Profumo, *Talanta,* 130 (2014) 90.
21. A. Fagan-Murphy, M.C. Allen, and B.A. Patel, *Electrochim. Acta,* 152 (2015) 249.
22. M. Taei, F. Hasanpour, H. Salavati, S.H. Banitaba, and F. Kazemi, *Mat. Sci. Eng. C-Mater.,* 59 (2016) 120.
23. F.P. Zhan, F. Gao, X. Wang, L.P. Xie, F. Gao, and Q.X. Wang, *Microchim. Acta,* 183 (2016) 1169.
24. L. Wang, and L. Xu, *J. Agr. Food. Chem.,* 62 (2016) 10248.
25. X.L. Ye, Y.L. Du, D.B. Lu, C.M. Wang, *Anal. Chim. Acta,* 779 (2013) 22-34.
26. W.Y. Wang, R.H. Li, X. Hua, R Zhang, *Electrochim. Acta,* 163 (2015) 48-56.
27. M. Pazalja, E. Kahrovic, A. Zahirovic, E. Turkusic, *Int. J. Electrochem. Sci.,* 11 (2016) 10939.
28. Z.H. Wang, H.J. Guo, R.J. Gui, H. Jin, J.F. Xia, F.F. Zhang, *Sensor. Actuat. B-chem.,* 255 (2018) 2069.
29. E. Boldenow, I. Hassan, M.C. Chames, C.W. Xi, and R. Loch-Caruso, *Reprod. toxicol.,* 52 (2015) 1.
30. J.L. Segura, M.J. Mancheño, and F. Zamora, *Chem. Soc. Rev.,* 45 (2016) 5635.
31. Y. Xiao, Y. Qin, M. Yi, and Y. Zhu, *J. Clust. Sci.,* 27 (2016) 1.
32. N. Nigam, S. Kumar, P.K. Dutta, S. Pei, and T. Ghosh, *Rsc. Adv.,* 6 (2016) 5575.
33. Y. Li, Y.H. Zhang, H.J. Niu, C. Wang, C.L. Qin, X.D. Bai, and W. Wang, *New. J. Chem.,* 40 (2016) 5245.
34. D. Sek, M. Siwy, M. Grucela, G. Malecki, E.M. Nowak, G. Lewinska, J. Santera, K. Laba M., Lapkowski, S. Kotowicz, and E. Schab-Balcerzak, *Spectrochim. Acta. A.* 175 (2017) 24.
35. C.Y. Sun, J.Y. Sun, P. Che, Z.D. Chang, W.J. Li, and F.Z. Qiu, *J. Lumin.,* 188 (2017) 246.
36. K Polat., M. Ucar, M.L. Aksu, and H. Unver, *Can. J. Chem.,* 82 (2004) 1150.
37. X.T. Wu, W. Wang, B. Li, Y.J. Hou, H.J. Niu, Y.H. Zhang, S.H. Wang, and X.D. Bai, *Spectrochim. Acta. A.,* 140 (2015) 398.
38. J.C. Lee, Y.K. Jeong, J.M. Kim, and J.G. Kang, *Spectrochim. Acta. A,* 124 (2014) 256.
39. A. Mashkoor, P. Caofeng, and Z. Jing, *J. Mater. Chem.*, 20 (2010) 7169.
40. K. Palanisamy, and J. S.Abraham. *Biosens. Bioelectron.*, 30 (2011) 276.
41. C.Y. Deng, J.H. Chen, X.L. Chen, M.D. Wang, Z. Nie, and S.Z. Yao. *Electrchim. Acta*, 54 (2009) 3298.
42. A.H. Kianfar, L. Kermat, M. Dostani, M. Shamsipur, M. Roushani, and F. Nikpour, *Spectrochim. Acta. A,* 77 (2010) 424.
43. D.F. Back, G.M.D. Oliveira, L.A. Fontana, B.F. Ramao, D. Roman, and B.A. Iglesias, *J. Mol. Struct.,* 1100 (2015) 264.
44. F.N.D. Kaya, I. Svoboda, O. Atakol, U. Ergun, A. Kenar, M. Sari, and K. C.Emregul, *J. Therm. Anal. Calorim.,* 92 (2008) 617.
45. C.M. Sharaby, M.F. Amine, and A.A. Asmaa, *J. Mol. Struct.*, 1134 (2017) 208.
46. N. Noori, M. Nikoorazm, and A. Ghorbani-Choghamarani, *Acta. Phys. Pol.-A.* 129 (2016) 208.
47. S. Rana, S.K. Mittal, N. Singh, J. Singh, and C.E. Banks, *Sensor. Actuat. B-Chem.*, 239 (2017) 17.
48. Y.L. Wei, A.T. Wang, and S.B. Wu, *J. New. Mat. Electr. Sys.*, 16 (2013) 65.
49. J.H. He, S.T. Zhang, Y.H. Cai, and Z.R. Song, *Asian. J. Chem.*, 25 (2013) 10121.
50. A. Mendez, S. Isikli, and R. Diaz, *Electrochemistry*, 81 (2013) 853.
51. K. Sipa, M. Brycht, A. Leniart, P. Urbaniak, and A. Nosal-Wiercińska, *Talanta*, 176 (2018) 625.

52. H. Kanso, M.B. González García, L.F. Llano, S. Ma, R. Ludwig, P.F. Bolado, and D.H. Santos, *Biosens. Bioelectron.*, 93 (2016) 298.
53. E. Sharifi, A. Salimi, and E. Shams, *Bioelectrochemistry*, 86 (2012) 9.
54. X.F. Tang, Y. Liu, H.Q. Hou, and T.Y. You, *Talanta,* 80 (2010) 2182.
55. H.F. L, L.L. Ye, Y.W. Wang, and C.G. Xie, *Microchim. Acta,* 185 (2018) 5
56. S. Sundaram, M.R.A. Kadir, A.S. Kumar, P. Nagamony, and V. Chinnuswamy, *Anal. Methods*, 9 (2017) 6791.